A case of torsion–tension in plasticity – analytical treatment and indirect approaches

IOANNIS DOLTSINIS
Institute of Statics and Dynamics of Aerospace Structures
Faculty of Aerospace Engineering and Geodesy
University of Stuttgart
Pfaffenwaldring 27, 70569 Stuttgart
GERMANY

Abstract: The plastic deformation of a thin-walled circular cylinder is considered for a specified sequence of torsion and tension. The case was originally intended for contrasting in general terms kinematic hardening with the isotropic hardening model. With the present account the analysis is accomplished presenting the closed-form solution for a linear yield stress and exploring approximations. In addition to the direct analytic treatment iterative procedures, numerical and successive functional update are investigated.

Key–Words: Plastic deformation, kinematic vs. isotropic hardening, closed-form solution, successive functional approach, numerical integration.

Received: March 22, 2025. Revised: June 15, 2025. Accepted: July 18, 2025. Published: November 14, 2025.

1 Introduction

Laboratory tests with thin-walled circular cylinders allow a multi-axial state of stress to be controlled by the applied loading: axial force, internal pressure, and torque. The experiment on plastic deformation considered here refers to a loading sequence of torsion, torsion/tension, and tension [1]. It was observed that in the last step of the sequence, the plastic twist obtained before decreases under tension. This observation, that could be predicted by the theory in [2] involving a displacement of the yield locus, has occasioned research regarding the constitutive representation partly controversial to the classical plasticity theory [3], [4], [5].

The formal interpretation of the experiment appears to be sensitive to the hardening model: while there is no conformity with the assumption of isotropic hardening, kinematic hardening is seen to predict the diminishing twist in the last step of the loading/unloading program. The case has been treated earlier in [6], to demonstrate the difference between the two hardening models in general terms. The present study develops analytical expressions for the plastic deformation during the entire course of the process. Dealing with isotropic hardening implies the evaluation of integrals while the kinematic counterpart requires the solution of ordinary differential equations, non-linearity included. In addition to the closed-form solution, approximations are considered as by a successive functional approach and by numerical integration; limitations of the latter are quantified.

An appraisal of the classical theory in the sense of plastic flow and isotropic hardening is presented in [7] performing the analysis of laboratory tests on thin tubes. Solutions, numerical and analytical, developed for a number of non-radial loading paths are contrasted with the results of experiments from other sources, the case under consideration not included.

The remainder of the account is organized as follows. Section 2 is concerned with the statement of the problem and definitions. Section 3 deals with the isotropic hardening model, Section 4 develops the solution for the kinematic hardening model. Indirect, approximate solution methods for the encountered differential equation are explored in Section 5 along with limitations for the numerical schemes. Conclusions regarding the plasticity aspect, the solution and the trial methods are subject of Section 6.

2 Problem statement and definitions

The thin-walled circular cylinder depicted in Fig. 1 is subjected to a loading program of torsion and tension. The load system is assumed to induce a homogeneous state of stress defined at each instant by the shear stress τ from torsion and the axial stress σ from tension. At each point of the wall, the stress

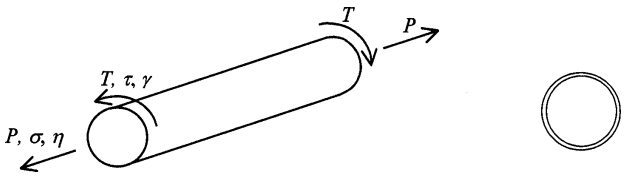

Figure 1: Thin-walled circular cylinder under tension and torsion. Source: created by the author.

state is referred to a system 0–r, t, z along the radial, circumferential, and axial direction. The non-zero components $\sigma_{\rm zz} = \sigma$ and $\sigma_{\rm tz} = \tau$ are collected in the 2×1 array (vector) $\boldsymbol{\sigma}$, the associated components of the deviatoric stress in $\boldsymbol{\sigma}_{\rm D}$, those of the plastic strain in the vector $\boldsymbol{\eta}$ where $\eta = \eta_{\rm zz}$ denotes the plastic strain in axial direction, and $\gamma = \eta_{\rm tz}$ is the shear strain. The collective representation is defined as

$$\boldsymbol{\sigma} = \begin{bmatrix} \sigma \\ \sqrt{2}\tau \end{bmatrix}, \boldsymbol{\sigma}_{\rm D} = \begin{bmatrix} \frac{2}{3}\sigma \\ \sqrt{2}\tau \end{bmatrix}, \boldsymbol{\eta} = \begin{bmatrix} \eta \\ \frac{1}{\sqrt{2}}\gamma \end{bmatrix}, \quad (1)$$

The lateral components of the deviatoric stress $\sigma_{\rm Drr} = \sigma_{\rm Dtt} = -\sigma/3$ missing in eqn (1) compensate the axial component $\sigma_{\rm Dzz} = 2\sigma/3$. The associated components of the plastic strain satisfy the isochoric condition such that with $\eta_{\rm zz} = \eta$: $\eta_{\rm rr} = \eta_{\rm tt} = -\eta/2$.

The equivalent deviatoric stress $\bar{\sigma}$ in terms of the applied stress σ and τ reads

$$\begin{aligned} \bar{\sigma}^2 &= \frac{3}{2}\left[\left(-\frac{\sigma}{3}\right)^2 + \left(-\frac{\sigma}{3}\right)^2 + \left(\frac{2\sigma}{3}\right)^2 + 2\tau^2\right] \\ &= \sigma^2 + 3\tau^2, \end{aligned} \quad (2)$$

and the equivalent plastic strain $\bar{\eta}$ in terms of η and γ is

$$\begin{aligned} \bar{\eta}^2 &= \frac{2}{3}\left[\left(-\frac{\eta}{2}\right)^2 + \left(-\frac{\eta}{2}\right)^2 + \eta^2 + \left(\frac{\gamma}{\sqrt{2}}\right)^2\right] \\ &= \eta^2 + \frac{1}{3}\gamma^2. \end{aligned} \quad (3)$$

3 The result of isotropic hardening

Isotropic hardening [8] restricts the equivalent deviatoric stress $\bar{\sigma}$ by the momentary yield stress $\sigma_{\rm f}$ of the material. The two quantities are set equal during the course of plastic flow; with eqn (2),

$$\bar{\sigma}^2 = \sigma^2 + 3\tau^2 = \sigma_{\rm f}^2. \quad (4)$$

This defines the yield locus as a circle of radius $\sigma_{\rm f}$ centered at the origin in the $\sigma, \sqrt{3}\tau$–plane (Fig. 2). The uniaxial tensile test is used to define the hardening law of the material as the functional dependence of

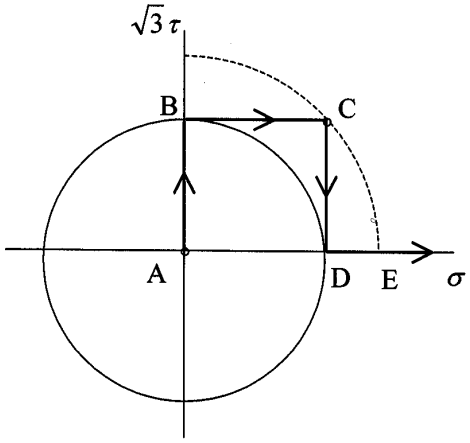

Figure 2: Isotropic hardening. Loading sequence and expanding yield locus of initial radius $\sigma_{\rm s}$. Source: created by the author.

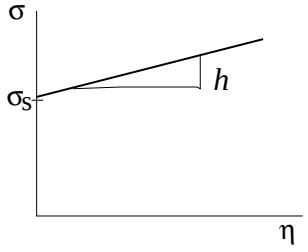

Figure 3: Linear hardening of plastic material. Source: created by the author.

the yield stress on the accumulated equivalent plastic strain

$$\sigma_{\rm f}(\bar{\eta}) \Leftarrow \sigma_{\rm f}(\eta), \quad \bar{\eta} = \int {\rm d}\bar{\eta}. \quad (5)$$

Equation (3) applies to ${\rm d}\bar{\eta}$ which accumulates to $\bar{\eta}$. Initially $\sigma_{\rm f}(\eta = 0) = \sigma_{\rm s}$, the elasticity limit of the material in tension.

From eqn (5), and on account of the equality by eqn (4),

$${\rm d}\bar{\eta} = \frac{1}{h}{\rm d}\sigma_{\rm f} = \frac{1}{h}{\rm d}\bar{\sigma}, \quad (6)$$

where h determines the increment of the yield stress in plastic straining. The following assumes throughout a linear increase for which $h =$ constant (Fig. 3). Thus the hardening law of the material becomes

$$\sigma_{\rm f} = \sigma_{\rm s} + h\bar{\eta}. \quad (7)$$

The flow rule states plastic deformation to occur along the deviatoric stress

$${\rm d}\boldsymbol{\eta} = \frac{3}{2}\frac{{\rm d}\bar{\eta}}{\bar{\sigma}}\boldsymbol{\sigma}_{\rm D}. \quad (8)$$

For the arrays $\boldsymbol{\sigma}_{\mathrm{D}}$ and $\boldsymbol{\eta}$ in eqn (1) and using eqn (6) for $\mathrm{d}\bar{\eta}$,

$$\begin{bmatrix} \mathrm{d}\eta \\ \frac{1}{\sqrt{2}}\mathrm{d}\gamma \end{bmatrix} = \frac{3}{2}\frac{1}{h}\frac{\mathrm{d}\bar{\sigma}}{\bar{\sigma}} \begin{bmatrix} \frac{2}{3}\sigma \\ \sqrt{2}\tau \end{bmatrix}. \tag{9}$$

From eqn (2) by differentiation,

$$\frac{\mathrm{d}\bar{\sigma}}{\bar{\sigma}} = \frac{\sigma\mathrm{d}\sigma + 3\tau\mathrm{d}\tau}{\sigma^2 + 3\tau^2} \Rightarrow \frac{\sigma\mathrm{d}\sigma}{\sigma^2 + 3\tau^2}. \tag{10}$$

The last expression realizes that plastic deformation evolves while the torque is kept constant in the loading sequence.

Following Fig. 2, the torque, applied first, is increased until the elasticity limit σ_{s} of the material (path A–B); no plastic flow occurs. At constant torque, the axial force is superposed progressing from zero (path B–C). Thereby plastic flow occurs and contributes to both elongation and twist of the cylinder. Integration of eqn (9) under observance of eqn (10) in the interval $[0, \sigma]$ at constant $\sqrt{3}\tau = \sigma_{\mathrm{s}}$ gives the plastic strain along the path B–C. In terms of standardized quantities,

$$\begin{bmatrix} \frac{h\eta}{\sigma_{\mathrm{s}}} \\ \frac{h\gamma}{\sqrt{3}\sigma_{\mathrm{s}}} \end{bmatrix} = \begin{bmatrix} \frac{1}{\sigma_{\mathrm{s}}}\int\limits_0^{\sigma} \frac{\sigma^2\mathrm{d}\sigma}{\sigma^2+\sigma_{\mathrm{s}}^2} \\ \int\limits_{\sigma_{\mathrm{s}}}^{\bar{\sigma}} \frac{\mathrm{d}\bar{\sigma}}{\bar{\sigma}} \end{bmatrix} = \begin{bmatrix} \frac{\sigma}{\sigma_{\mathrm{s}}} - \arctan\frac{\sigma}{\sigma_{\mathrm{s}}} \\ \frac{1}{2}\ln\left(1 + \frac{\sigma^2}{\sigma_{\mathrm{s}}^2}\right) \end{bmatrix}. \tag{11}$$

At point C ($\sigma = \sqrt{3}\tau = \sigma_{\mathrm{s}}$),

$$\begin{bmatrix} \frac{h\eta}{\sigma_{\mathrm{s}}} \\ \frac{h\gamma}{\sqrt{3}\sigma_{\mathrm{s}}} \end{bmatrix}_{\mathrm{C}} = \begin{bmatrix} 1 - \frac{\pi}{4} = 0.21460 \\ \frac{1}{2}\ln 2 = 0.34657 \end{bmatrix}. \tag{12}$$

The evolution of the plastic strain, extension and shear, under the combined action of tension and torsion along the path B–C is plotted in Fig. 4 as a function of the progressing tensile stress. The flow rule, eqn (9), relates the rate of change of the two strain components

$$\begin{aligned} \frac{1}{\sqrt{3}}\frac{\mathrm{d}\gamma}{\mathrm{d}\eta} &= \frac{\sqrt{3}\tau}{\sigma}, \\ \left(\frac{1}{\sqrt{3}}\frac{\mathrm{d}\gamma}{\mathrm{d}\eta}\right)_{\mathrm{B}} &= \infty, \quad \left(\frac{1}{\sqrt{3}}\frac{\mathrm{d}\gamma}{\mathrm{d}\eta}\right)_{\mathrm{C}} = 1. \end{aligned} \tag{13}$$

Elimination in eqn (11) of the stress term between upper and lower raw leaves a relation between axial and shear strain as displayed in Fig. 5

$$\begin{aligned} \frac{h\eta}{\sigma_{\mathrm{s}}} &= \left(\exp\frac{2h\gamma}{\sqrt{3}\sigma_{\mathrm{s}}} - 1\right)^{\frac{1}{2}} \\ &- \arctan\left(\exp\frac{2h\gamma}{\sqrt{3}\sigma_{\mathrm{s}}} - 1\right)^{\frac{1}{2}}. \end{aligned} \tag{14}$$

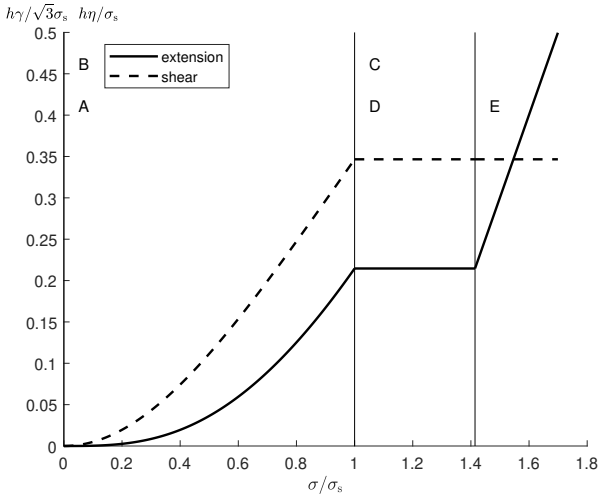

Figure 4: Isotropic hardening. Plastic extension and shear as functions of the progressing tensile stress. Source: created on behalf of the author.

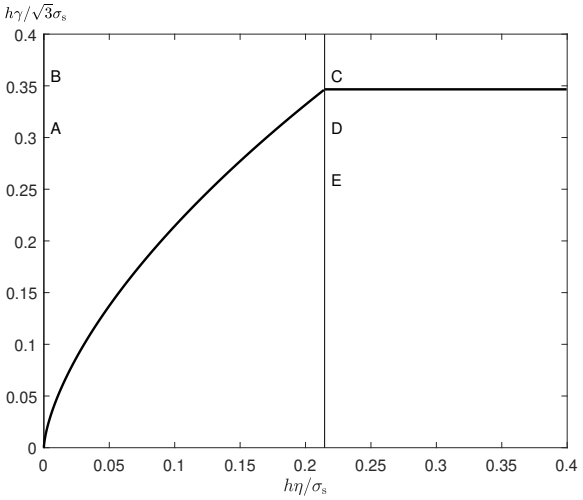

Figure 5: Isotropic hardening. Mutual evolution of shear- and axial strain. Source: created on behalf of the author.

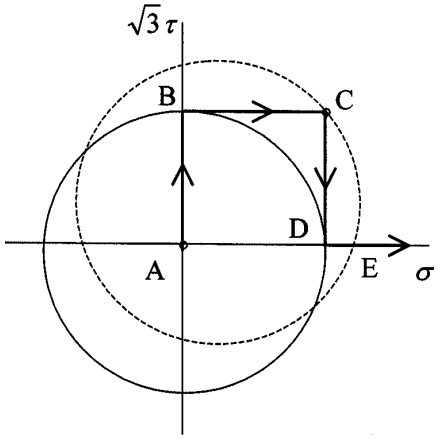

Figure 6: Kinematic hardening. Loading sequence and displaced yield locus of radius $\sigma_{\rm s}$. Source: created by the author.

Plastic deformation augments the yield stress of the material in compliance with the scalar equivalent of the imposed deviatoric stress. Equation (4) defines the momentary extent of the circular yield locus. Since $\sqrt{3}\tau = \sigma_{\rm s}$,

$$\left(\frac{\sigma_{\rm f}}{\sigma_{\rm s}}\right)_{\rm B-C} = \sqrt{1+\left(\frac{\sigma}{\sigma_{\rm s}}\right)^2}, \qquad (15)$$
$$\left(\frac{\sigma_{\rm f}}{\sigma_{\rm s}}\right)_{\rm B} = 1, \quad \left(\frac{\sigma_{\rm f}}{\sigma_{\rm s}}\right)_{\rm C} = \sqrt{2}.$$

Alternatively from the hardening postulate for the material in eqn (7),

$$\left(\frac{\sigma_{\rm f}}{\sigma_{\rm s}}\right) = 1+\sqrt{\left(\frac{h\eta}{\sigma_{\rm s}}\right)^2+\frac{1}{3}\left(\frac{h\gamma}{\sigma_{\rm s}}\right)^2}. \qquad (16)$$

Removal of the torque at constant tension (path C–D) leaves the plastic deformation unchanged. Loading along D–E progresses alone under tension $(\tau = 0, \sigma)$. Plastic flow that occurs once the stress σ surpasses the yield locus at point E merely adds to the direct plastic strain: $\eta = \eta_{\rm C} + (\sigma - \sigma_{\rm f,C})/h$ as from the uniaxial stress–plastic strain characteristic. Thus

$$\begin{bmatrix} \frac{h\eta}{\sigma_{\rm s}} \\ \frac{h\gamma}{\sqrt{3}\sigma_{\rm s}} \end{bmatrix}_{\rm E+} = \begin{bmatrix} \left(\frac{h\eta}{\sigma_{\rm s}}\right)_{\rm C} + \frac{\sigma}{\sigma_{\rm s}} - \left(\frac{\sigma_{\rm f}}{\sigma_{\rm s}}\right)_{\rm C} \\ \left(\frac{h\gamma}{\sqrt{3}\sigma_{\rm s}}\right)_{\rm C} \end{bmatrix}, \qquad (17)$$

which completes Fig. 4. The values of the variables at point C are as in eqn (12) and eqn (15).

4 Solution for kinematic hardening

The loading sequence is as before with isotropic hardening. The kinematic model [9] effects a translation of the yield locus keeping it unaltered while plastic deformation progresses (Fig. 6). In what follows the translation is defined in the deviatoric stress space by the essential components $\alpha_{\rm zz} = \alpha$ and $\alpha_{\rm tz} = \beta$. The lateral components $\alpha_{\rm rr} = \alpha_{\rm tt} = -\alpha/2$ do not appear in the collective vector representation

$$\boldsymbol{\alpha} = \begin{bmatrix} \alpha \\ \sqrt{2}\beta \end{bmatrix} = \frac{2}{3}h\begin{bmatrix} \eta \\ \frac{1}{\sqrt{2}}\gamma \end{bmatrix}. \qquad (18)$$

The quantities α and β act as the hardening variables that evolve with plastic deformation. The due relationship, originally infinitesimal, transforms to the above finite values on account of the assumption $h =$ constant.

The deviatoric stress quantity assumed relevant to plasticity is measured from the displaced origin. This relative deviatoric stress is

$$\boldsymbol{\sigma}_{\rm KD} = \boldsymbol{\sigma}_{\rm D} - \boldsymbol{\alpha}. \qquad (19)$$

The scalar equivalent $\bar{\sigma}_{\rm K}$ is defined in analogy to $\bar{\sigma}$ in eqn (2). It is restricted by the elasticity limit $\sigma_{\rm s}$ of the material in tension

$$\bar{\sigma}_{\rm K}^2 = \frac{3}{2}\left[\left(\frac{\sigma}{3}-\frac{\alpha}{2}\right)^2+\left(\frac{\sigma}{3}-\frac{\alpha}{2}\right)^2 + \left(\frac{2\sigma}{3}-\alpha\right)^2+2(\tau-\beta)^2\right] = $$
$$= \left(\sigma-\frac{3}{2}\alpha\right)^2+3(\tau-\beta)^2 = \sigma_{\rm s}^2. \qquad (20)$$

The last fashion of eqn (20) specifies the yield locus in the $\sigma, \sqrt{3}\tau$–plane as a circle of radius $\sigma_{\rm s}$ with the center at $\sigma = 3\alpha/2, \sqrt{3}\tau = \sqrt{3}\beta$. Initially $\alpha = \beta = 0$ (Fig. 6).

The theory assumes here plastic deformation to progress along the relative deviatoric stress. Analogously to eqn (8)

$$\mathrm{d}\boldsymbol{\eta} = \frac{3}{2}\frac{\mathrm{d}\bar{\eta}}{\bar{\sigma}_{\rm K}}\boldsymbol{\sigma}_{\rm KD}, \qquad (21)$$

and in detail

$$\begin{bmatrix} \mathrm{d}\eta \\ \frac{1}{\sqrt{2}}\mathrm{d}\gamma \end{bmatrix} = \frac{3}{2}\frac{\mathrm{d}\bar{\eta}}{\bar{\sigma}_{\rm K}}\begin{bmatrix} \frac{2}{3}\sigma-\alpha \\ \sqrt{2}(\tau-\beta) \end{bmatrix} = $$
$$= \frac{\mathrm{d}\bar{\eta}}{\sigma_{\rm s}}\begin{bmatrix} \sigma-h\eta \\ \frac{1}{\sqrt{2}}(3\tau-h\gamma) \end{bmatrix}. \qquad (22)$$

Changes of the stress that induce plastic flow effect a translation of the rigid yield locus in the $\sigma, \sqrt{3}\tau$–plane via α, β constrained by eqn (20). Differentiation there of the last equality and use of the hardening relation,

eqn (18), for the emerging variations in α and β along with eqn (22) for the incremental plastic strain gives an equation for the magnitude $\mathrm{d}\bar{\eta}$

$$\begin{aligned} h\sigma_{\mathrm{s}}\mathrm{d}\bar{\eta} &= \left(\sigma - \frac{3}{2}\alpha\right)\mathrm{d}\sigma + 3(\tau-\beta)\mathrm{d}\tau \\ &= (\sigma - h\eta)\mathrm{d}\sigma + (3\tau - h\gamma)\mathrm{d}\tau \\ &\Rightarrow (\sigma - h\eta)\mathrm{d}\sigma. \end{aligned} \tag{23}$$

Actually plastic flow occurs in the loading sequence while τ = constant which justifies in the above the reduction to the last expression. Substitution in eqn (22) completes the equation governing the plastic strain in tension and shear. In standardized form

$$\begin{bmatrix} \mathrm{d}\left(\frac{h\eta}{\sigma_{\mathrm{s}}}\right) \\ \mathrm{d}\left(\frac{h\gamma}{\sqrt{3}\sigma_{\mathrm{s}}}\right) \end{bmatrix} = \begin{bmatrix} \left(\frac{\sigma}{\sigma_{\mathrm{s}}} - \frac{h\eta}{\sigma_{\mathrm{s}}}\right)^2 \mathrm{d}\left(\frac{\sigma}{\sigma_{\mathrm{s}}}\right) \\ \left(\frac{\sqrt{3}\tau}{\sigma_{\mathrm{s}}} - \frac{h\gamma}{\sqrt{3}\sigma_{\mathrm{s}}}\right)\left(\frac{\sigma}{\sigma_{\mathrm{s}}} - \frac{h\eta}{\sigma_{\mathrm{s}}}\right)\mathrm{d}\left(\frac{\sigma}{\sigma_{\mathrm{s}}}\right) \end{bmatrix}. \tag{24}$$

4.1 The path B–C

Application of the torque along the path A–B is within the elastic range. Superposition of the axial force along the path B–C ($\sigma = [0, \sigma_{\mathrm{s}}]$, $\sqrt{3}\tau = \sigma_{\mathrm{s}}$), induces plastic flow contributing to both elongation and twist of the tube. The evolution of the tensile strain (upper row in eqn (24)) requires treatment of a differential equation of the form

$$\mathrm{d}y = (x-y)^2\mathrm{d}x, \tag{25}$$

with the abbreviations

$$y = \frac{h\eta}{\sigma_{\mathrm{s}}}, \quad x = \frac{\sigma}{\sigma_{\mathrm{s}}}. \tag{26}$$

The solution makes use of the auxiliary variable, [10],

$$\begin{aligned} u &= x - y \\ \mathrm{d}u &= (1-u^2)\mathrm{d}x \end{aligned} \tag{27}$$

Integrating after separation of the variables,

$$\begin{aligned} \int_0^u \frac{\mathrm{d}u}{1-u^2} &= \int_0^u \frac{1}{2}\left(\frac{1}{1-u} + \frac{1}{1+u}\right)\mathrm{d}u \\ &= \frac{1}{2}\ln\frac{1+u}{1-u} = \int_0^x \mathrm{d}x = x - 0. \end{aligned} \tag{28}$$

Therefrom observing the definition of u by eqn (27)

$$u = \frac{e^{2x}-1}{e^{2x}+1} = x - y, \quad y = x - \frac{e^{2x}-1}{e^{2x}+1}. \tag{29}$$

It is noticed that $0 \le x$ gives $-1 \le u$ which ensures the existence of the logarithm in eqn (28).

The plastic shear (lower row in eqn (24) with $\sqrt{3}\tau = \sigma_{\mathrm{s}}$) suggests separate arrangement of homologous variables and evaluation of two integrals. Symbolically using x and y as before along with the abbreviation

$$z = \frac{h\gamma}{\sqrt{3}\sigma_{\mathrm{s}}}, \tag{30}$$

one obtains

$$\int_0^z \frac{\mathrm{d}z}{1-z} = \int_0^x (x-y)\mathrm{d}x. \tag{31}$$

The right-hand side takes advantage of eqn (29) from the previous solution in expressing the integrand as a function of x to give

$$\begin{aligned} \int_0^x (x-y)\mathrm{d}x &= \int_0^x \frac{e^{2x}-1}{e^{2x}+1}\mathrm{d}x \\ &= \int_0^x \left(\frac{2e^{2x}}{e^{2x}+1} - 1\right)\mathrm{d}x \\ &= \int_0^x \frac{\mathrm{d}(e^{2x}+1)}{e^{2x}+1} - \int_0^x \mathrm{d}x \\ &= \ln\frac{e^{2x}+1}{2} - x. \end{aligned} \tag{32}$$

The other integral refers to the left-hand side of the differential shear after separation of the variables

$$\int_0^z \frac{\mathrm{d}z}{1-z} = -\ln(1-z). \tag{33}$$

Equating the results of eqn (32) and eqn (33)

$$z = 1 - \frac{2e^x}{1+e^{2x}} = \frac{(1-e^x)^2}{1+e^{2x}}. \tag{34}$$

Interpretation of $y(x)$ in eqn (29) and $z(x)$ in eqn (34) for the original quantities appearing in eqn (24) specifies the functional dependence of the axial strain on the tensile stress and so of the shear strain as follows

$$\begin{bmatrix} \frac{h\eta}{\sigma_{\mathrm{s}}} \\ \frac{h\gamma}{\sqrt{3}\sigma_{\mathrm{s}}} \end{bmatrix} = \begin{bmatrix} \frac{\sigma}{\sigma_{\mathrm{s}}} + \frac{1-\exp\left(2\frac{\sigma}{\sigma_{\mathrm{s}}}\right)}{1+\exp\left(2\frac{\sigma}{\sigma_{\mathrm{s}}}\right)} \\ 1 - \frac{2\exp\left(\frac{\sigma}{\sigma_{\mathrm{s}}}\right)}{1+\exp\left(2\frac{\sigma}{\sigma_{\mathrm{s}}}\right)} = \frac{\left[1-\exp\left(\frac{\sigma}{\sigma_{\mathrm{s}}}\right)\right]^2}{1+\exp\left(2\frac{\sigma}{\sigma_{\mathrm{s}}}\right)} \end{bmatrix}. \tag{35}$$

Figure 7 shows the evolution of the plastic strain along the path B–C. At point C ($\sigma = \sigma_{\mathrm{s}}$, $\sqrt{\tau} = \sigma_{\mathrm{s}}$),

$$\begin{bmatrix} \frac{h\eta}{\sigma_{\mathrm{s}}} \\ \frac{h\gamma}{\sqrt{3}\sigma_{\mathrm{s}}} \end{bmatrix}_{\mathrm{C}} = \begin{bmatrix} \frac{2}{1+e^2} \\ 1 - \frac{2e}{1+e^2} = \frac{(1-e)^2}{1+e^2} \end{bmatrix} = \begin{bmatrix} 0.23840 \\ 0.35194 \end{bmatrix}. \tag{36}$$

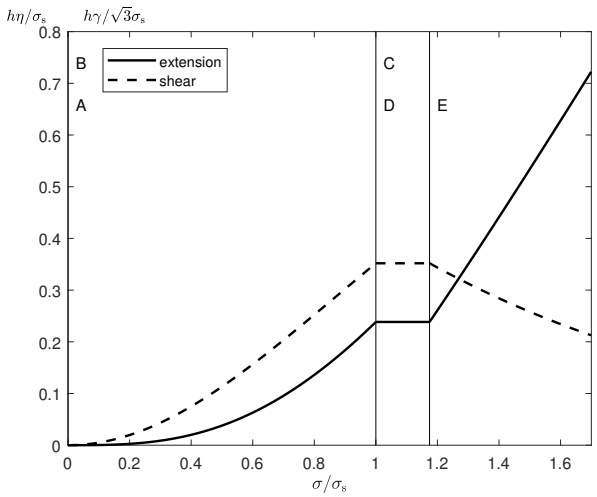

Figure 7: Kinematic hardening. Plastic extension and shear as functions of the progressing tensile stress. Source: created on behalf of the author.

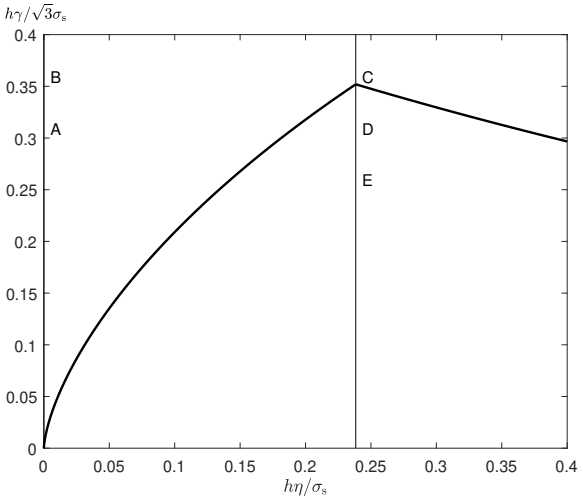

Figure 8: Kinematic hardening. Mutual evolution of shear- and axial strain. Source: created on behalf of the author.

Plastic deformation has displaced the circular yield locus. At point C of the loading sequence the position of the translated center is

$$\begin{bmatrix} \frac{\alpha}{\sigma_s} \\ \frac{\sqrt{3}\beta}{\sigma_s} \end{bmatrix}_C = \begin{bmatrix} \frac{2}{3}\frac{h\eta}{\sigma_s} \\ \frac{h\gamma}{\sqrt{3}\sigma_s} \end{bmatrix}_C = \begin{bmatrix} 0.15893 \\ 0.35194 \end{bmatrix}. \quad (37)$$

The translation is seen more pronounced along the shear stress which dominates in fact the plastic flow while the normal stress is progressing.

4.2 Beyond point E

The torque is removed along C–D (Fig. 6). The subsequent increase of the tensile force does not activate plastic flow until the stress attains the yield locus at point E. Evaluation of eqn (20) at the actual position of the displaced yield locus, α_C, β_C from eqn (37), determines the stress σ at the intersection with the axis where $\tau = 0$

$$\left(\sigma_E - \frac{3}{2}\alpha_C\right)^2 + 3\beta_C^2 = \sigma_s^2,$$

$$\frac{\sigma_E}{\sigma_s} = \frac{3}{2}\frac{\alpha_C}{\sigma_s} + \sqrt{1 - 3\left(\frac{\beta_C}{\sigma_s}\right)^2} = 1.1744263. \quad (38)$$

Beyond point E ($\sigma \geq \sigma_E, \tau = 0$) the progress in axial strain, eqn (24), allows treatment as for eqn (25). The integration by the auxiliary variable $u = x - y$ as in eqn (28) observes the due limits

$$\int_{u_0}^{u} \frac{du}{1-u^2} = \frac{1}{2}\ln\frac{(1+u)(1-u_0)}{(1-u)(1+u_0)} = \int_{x_0}^{x} dx = x - x_0. \quad (39)$$

Therefrom

$$u = \frac{(1+u_0)e^{2(x-x_0)} - (1-u_0)}{(1+u_0)e^{2(x-x_0)} + (1-u_0)} = x - y. \quad (40)$$

In terms of the original variables eqn (40) determines the axial strain as a function of the tensile stress beyond point E:

$$\frac{h\eta}{\sigma_s} = \frac{\sigma}{\sigma_s} + \quad (41)$$

$$\frac{\left(1 - \frac{\sigma_E}{\sigma_s} + \frac{h\eta_E}{\sigma_s}\right) - \left(1 + \frac{\sigma_E}{\sigma_s} - \frac{h\eta_E}{\sigma_s}\right)\exp 2\left(\frac{\sigma}{\sigma_s} - \frac{\sigma_E}{\sigma_s}\right)}{\left(1 - \frac{\sigma_E}{\sigma_s} + \frac{h\eta_E}{\sigma_s}\right) + \left(1 + \frac{\sigma_E}{\sigma_s} - \frac{h\eta_E}{\sigma_s}\right)\exp 2\left(\frac{\sigma}{\sigma_s} - \frac{\sigma_E}{\sigma_s}\right)}.$$

The plastic shear evolves with $\tau = 0$ in eqn (22) while β is active. The absence of the shear stress affects eqn (24) such that eqn (31) becomes

$$\int_{z_0}^{z} -\frac{dz}{z} = \int_{x_0}^{x} (x-y)dx, \quad (42)$$

to be evaluated for the actual limits. The left-hand side gives

$$\int_{z_0}^{z} -\frac{dz}{z} = -\ln\frac{z}{z_0}. \quad (43)$$

The integrand on the right-hand side is from eqn (40). Executing the integration analogously to eqn (32),

$$\int_{x_0}^{x} (x-y)dx = \int_{x_0}^{x} \frac{(1+u_0)e^{2(x-x_0)} - (1-u_0)}{(1+u_0)e^{2(x-x_0)} + (1-u_0)}dx =$$

$$= \int_{x_0}^{x} \frac{\mathrm{d}\left((1+u_0)e^{2(x-x_0)} + (1-u_0)\right)}{(1+u_0)e^{2(x-x_0)} + (1-u_0)} - \int_{x_0}^{x} \mathrm{d}x$$
$$= \ln \frac{(1+u_0)e^{2(x-x_0)} + (1-u_0)}{2} - (x-x_0). \tag{44}$$

The equality of eqn (43) with eqn (44) determines the substitute z of the shear strain

$$\frac{z}{z_0} = \frac{2e^{(x-x_0)}}{(1-u_0) + (1+u_0)e^{2(x-x_0)}}. \tag{45}$$

In terms of the original variables eqn (45) describes the shear strain as a decaying function of the surplus axial stress; in the standardized notation

$$\frac{\gamma}{\gamma_\mathrm{E}} = \tag{46}$$
$$\frac{2\exp\left(\frac{\sigma}{\sigma_\mathrm{s}} - \frac{\sigma_\mathrm{E}}{\sigma_\mathrm{s}}\right)}{\left(1 - \frac{\sigma_\mathrm{E}}{\sigma_\mathrm{s}} + \frac{h\eta_\mathrm{E}}{\sigma_\mathrm{s}}\right) + \left(1 + \frac{\sigma_\mathrm{E}}{\sigma_\mathrm{s}} - \frac{h\eta_\mathrm{E}}{\sigma_\mathrm{s}}\right)\exp 2\left(\frac{\sigma}{\sigma_\mathrm{s}} - \frac{\sigma_\mathrm{E}}{\sigma_\mathrm{s}}\right)}.$$

Equation (41) defines the evolution of the axial strain for the tensile stress beyond point E, as does eqn (46) for the shear strain. Either variation is plotted in Fig. 7. It is noted that at point E the strain variables stay at the values of point C given in eqn (36) and the stress variable assumes the value computed in eqn (38).

In the present case the flow rule defines the rate of change of the two strain quantities as

$$\frac{1}{\sqrt{3}}\frac{\mathrm{d}\gamma}{\mathrm{d}\eta} = \frac{\sqrt{3}(\tau-\beta)}{\sigma - \frac{3}{2}\alpha}, \tag{47}$$

which is but the slope of the curve in Fig. 8 showing the variation of the shear while the tube is extending. With eqn (47) the displacement of the rigid yield locus is seen to be along

$$\frac{\mathrm{d}\beta}{\mathrm{d}\alpha} = \frac{1}{2}\frac{\mathrm{d}\gamma}{\mathrm{d}\eta} = \frac{3}{2}\frac{\tau-\beta}{\sigma - \frac{3}{2}\alpha}. \tag{48}$$

In Fig. 9 the mutual evolution of shear and extension under kinematic hardening is contrasted with the isotropic one.

5 Approximate analysis

Approximate analysis will focus on the plastic deformation along the loading path B–C as for kinematic hardening. The task regarding the integration of the solution of the governing differential equation is handled numerically as well as analytically were appropriate.

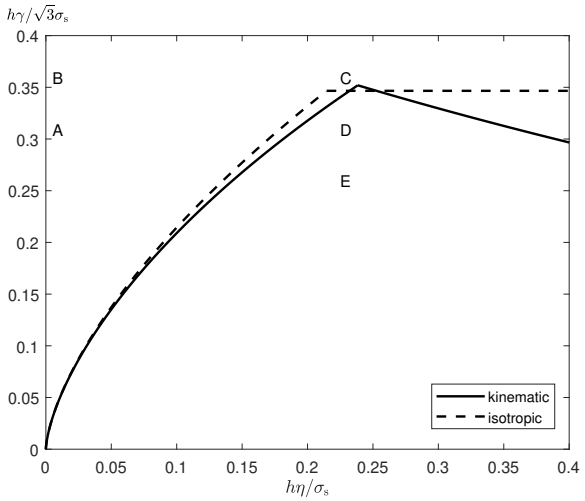

Figure 9: Contrasting isotropic with kinematic hardening in terms of mutually evolving deformation. Source: created on behalf of the author.

5.1 Axial strain

5.1.1 Numerical treatment

The computation of the axial strain along B–C for the kinematic hardening model requires integration of the upper row in eqn (24). Incrementation effects the transition from stage n to $n+1$

$$\left(\frac{h\eta}{\sigma_\mathrm{s}}\right)_{n+1} =$$
$$= \left(\frac{h\eta}{\sigma_\mathrm{s}}\right)_n + \int_n^{n+1} \left(\frac{\sigma}{\sigma_\mathrm{s}} - \frac{h\eta}{\sigma_\mathrm{s}}\right)^2 \mathrm{d}\left(\frac{\sigma}{\sigma_\mathrm{s}}\right). \tag{49}$$

Approximately,

$$\left(\frac{h\eta_{i+1}}{\sigma_\mathrm{s}}\right)_{n+1} =$$
$$= \left(\frac{h\eta}{\sigma_\mathrm{s}}\right)_n + \left(\frac{\sigma}{\sigma_\mathrm{s}} - \frac{h\eta_i}{\sigma_\mathrm{s}}\right)_\zeta^2 \left(\frac{\sigma}{\sigma_\mathrm{s}}\right)_\Delta. \tag{50}$$

The presence of the unknown in the integrand suggests the recursive updating $i, i+1$. The integrand is taken as a linear combination of start- and end-value in the increment weighted by the collocation parameter $0 \le \zeta \le 1$

$$\left(\frac{\sigma}{\sigma_\mathrm{s}} - \frac{h\eta}{\sigma_\mathrm{s}}\right)_\zeta =$$
$$= (1-\zeta)\left(\frac{\sigma}{\sigma_\mathrm{s}} - \frac{h\eta}{\sigma_\mathrm{s}}\right)_n + \zeta\left(\frac{\sigma}{\sigma_\mathrm{s}} - \frac{h\eta}{\sigma_\mathrm{s}}\right)_{n+1}. \tag{51}$$

The stress is updated incrementally

$$\left(\frac{\sigma}{\sigma_\mathrm{s}}\right)_{n+1} = \left(\frac{\sigma}{\sigma_\mathrm{s}}\right)_n + \left(\frac{\sigma}{\sigma_\mathrm{s}}\right)_\Delta. \tag{52}$$

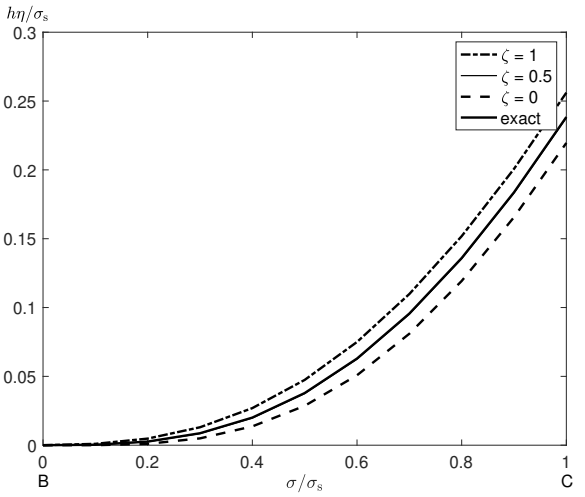

Figure 10: Incremental integration of the axial strain in kinematic hardening along B–C. Source: created on behalf of the author.

Results of the numerical procedure when advancing the standardized stress in the interval [0, 1] by ten equal increments are displayed in Fig. 10. The iteration converges to five digits within four to five cycles. In the figure the results for $\zeta = 0$ (explicit), $\zeta = 1$ (implicit) are contrasted with the analytical solution of eqn (35) which is fairly approximated by $\zeta = 1/2$ (second order).

5.1.2 Limitations

With regard to convergence, the variation of consecutive iterates from eqn (50) in conjunction with eqn (51) is

$$\delta\left(\frac{h\eta_{i+1}}{\sigma_s}\right)_{n+1} = \delta\left[\left(\frac{\sigma}{\sigma_s}-\frac{h\eta_i}{\sigma_s}\right)_\zeta^2\right]\left(\frac{\sigma}{\sigma_s}\right)_\Delta = \\ = -2\zeta\left(\frac{\sigma}{\sigma_s}-\frac{h\eta_i}{\sigma_s}\right)_\zeta \delta\left(\frac{h\eta_i}{\sigma_s}\right)_{n+1}\left(\frac{\sigma}{\sigma_s}\right)_\Delta . \quad (53)$$

Therefrom the convergence requirement

$$\left|\frac{\delta\eta_{i+1}}{\delta\eta_i}\right|_{n+1} = 2\zeta\left(\frac{\sigma}{\sigma_s}-\frac{h\eta_i}{\sigma_s}\right)_\zeta\left(\frac{\sigma}{\sigma_s}\right)_\Delta < 1, \quad (54)$$

which restricts the stress increment to

$$\left(\frac{\sigma}{\sigma_s}\right)_\Delta < \frac{1}{2\zeta}\left(\frac{\sigma}{\sigma_s}-\frac{h\eta_i}{\sigma_s}\right)_\zeta^{-1} . \quad (55)$$

Handling on the differential level simplifies reasoning, but the actual procedure involves differences such that

$$\delta\eta_{i+1} \Leftarrow \eta_{i+1}-\eta_i,\ \delta\eta_i \Leftarrow \eta_i-\eta_{i-1}.$$

This suggests the modification

$$(\eta_i)_\zeta \Leftarrow \frac{1}{2}(\eta_i+\eta_{i-1})_\zeta,$$

on the right-hand side of eqn (54).

Stability of the integration relates to the propagation of disturbances by the approximation scheme. From eqns (50), (51) by differentiation at constant stress,

$$\delta\left(\frac{h\eta}{\sigma_s}\right)_{n+1} = \delta\left(\frac{h\eta}{\sigma_s}\right)_n + \delta\left[\left(\frac{\sigma}{\sigma_s}-\frac{h\eta}{\sigma_s}\right)_\zeta^2\right]\left(\frac{\sigma}{\sigma_s}\right)_\Delta$$

$$= \delta\left(\frac{h\eta}{\sigma_s}\right)_n - 2\left(\frac{\sigma}{\sigma_s}-\frac{h\eta}{\sigma_s}\right)_\zeta \times \\ \times\left[(1-\zeta)\delta\left(\frac{h\eta}{\sigma_s}\right)_n + \zeta\delta\left(\frac{h\eta}{\sigma_s}\right)_{n+1}\right]\left(\frac{\sigma}{\sigma_s}\right)_\Delta . \quad (56)$$

Therefrom the stability requirement

$$\left|\frac{\delta\eta_{n+1}}{\delta\eta_n}\right| = \\ \left|\frac{1-2(1-\zeta)\left(\frac{\sigma}{\sigma_s}-\frac{h\eta}{\sigma_s}\right)_\zeta\left(\frac{\sigma}{\sigma_s}\right)_\Delta}{1+2\zeta\left(\frac{\sigma}{\sigma_s}-\frac{h\eta}{\sigma_s}\right)_\zeta\left(\frac{\sigma}{\sigma_s}\right)_\Delta}\right| < 1. \quad (57)$$

Assuming the parentheses in the denominator to be positive non-zero, this restricts the stress increment to

$$\left(\frac{\sigma}{\sigma_s}\right)_\Delta < \frac{1}{1-2\zeta}\left(\frac{\sigma}{\sigma_s}-\frac{h\eta}{\sigma_s}\right)_\zeta^{-1} . \quad (58)$$

Interpretation of eqn (56) for the differences between consecutive steps shows that oscillatory results are avoided if

$$\frac{\delta\eta_{n+1}}{\delta\eta_n} > 0, \\ \left(\frac{\sigma}{\sigma_s}\right)_\Delta < \frac{1}{2(1-\zeta)}\left(\frac{\sigma}{\sigma_s}-\frac{h\eta}{\sigma_s}\right)_\zeta^{-1} . \quad (59)$$

The effect of the collocation parameter ζ on the limitation of the stress increment is summarized in Fig. 11. The findings conform with the results of previous considerations in [11].

5.1.3 Functional approximation

The functional dependence of the axial strain on the stress is noted

$$\frac{h\eta}{\sigma_s} = f\left(\frac{\sigma}{\sigma_s}\right) . \quad (60)$$

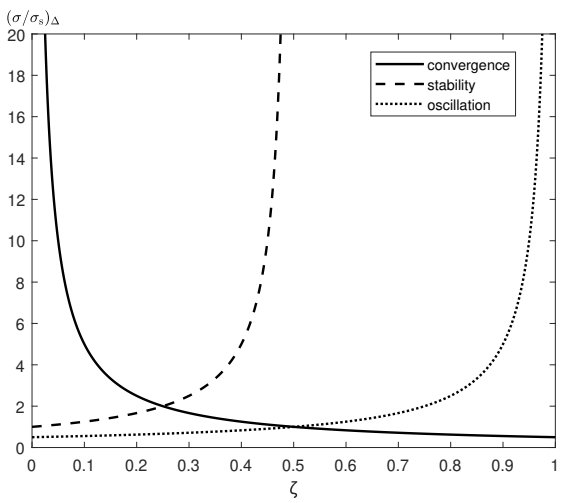

Figure 11: Limitation of incremental integration. Source: created on behalf of the author.

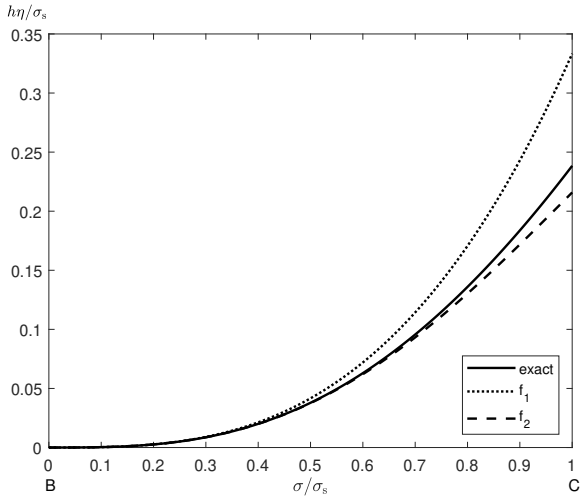

Figure 12: Successive analytical approximation for the axial strain in kinematic hardening along B–C. Source: created on behalf of the author.

The following attempt to search for the unknown function makes use of a successive approximation adapted from [12]. With reference to eqn (60) the integration in eqn (24) of the axial strain along the path B–C is stated in the recursive form

$$f_{i+1}\left(\frac{\sigma}{\sigma_\mathrm{s}}\right)=\int_0^{\frac{\sigma}{\sigma_\mathrm{s}}}\left[\frac{\sigma}{\sigma_\mathrm{s}}-f_i\left(\frac{\sigma}{\sigma_\mathrm{s}}\right)\right]^2\mathrm{d}\left(\frac{\sigma}{\sigma_\mathrm{s}}\right),\quad(61)$$

Starting with zero as an input for the function to find, the scheme gives consecutively

$$\begin{aligned}
f_0\left(\frac{\sigma}{\sigma_\mathrm{s}}\right) &= 0\\
f_1\left(\frac{\sigma}{\sigma_\mathrm{s}}\right) &= \frac{1}{3}\left(\frac{\sigma}{\sigma_\mathrm{s}}\right)^3,\\
f_2\left(\frac{\sigma}{\sigma_\mathrm{s}}\right) &= \frac{1}{3}\left(\frac{\sigma}{\sigma_\mathrm{s}}\right)^3-\frac{2}{15}\left(\frac{\sigma}{\sigma_\mathrm{s}}\right)^5+\frac{1}{63}\left(\frac{\sigma}{\sigma_\mathrm{s}}\right)^7,\\
f_3\left(\frac{\sigma}{\sigma_\mathrm{s}}\right) &= \cdots.
\end{aligned}\quad(62)$$

Fig. 12 compares to the solution, eqn (35).

5.2 Shear strain

5.2.1 Numerical integration

The plastic shear strain associated to kinematic hardening along B–C satisfies the equality of the integrals on the two sides in eqn (31). Using original variables in the incremental evaluation $n, n+1$,

$$\int_n^{n+1}\left(1-\frac{h\gamma}{\sigma_\mathrm{s}}\right)^{-1}\mathrm{d}\left(\frac{h\gamma}{\sigma_\mathrm{s}}\right)=$$

$$=\int_n^{n+1}\left(\frac{\sigma}{\sigma_\mathrm{s}}-\frac{h\eta}{\sigma_\mathrm{s}}\right)\mathrm{d}\left(\frac{\sigma}{\sigma_\mathrm{s}}\right).\quad(63)$$

The approximated increment of the left-hand side is set equal to that of the right-hand side

$$\left(1-\frac{h\gamma}{\sigma_\mathrm{s}}\right)_\zeta^{-1}\left(\frac{h\gamma}{\sigma_\mathrm{s}}\right)_\Delta=R_\Delta.\quad(64)$$

The right-hand side takes recourse of the axial strain computed before

$$R_\Delta=\left(\frac{\sigma}{\sigma_\mathrm{s}}-\frac{h\eta}{\sigma_\mathrm{s}}\right)_\zeta\left(\frac{\sigma}{\sigma_\mathrm{s}}\right)_\Delta\quad(65)$$

Noting that in eqn (64)

$$\left(\frac{h\gamma}{\sigma_\mathrm{s}}\right)_\Delta=\left(\frac{h\gamma}{\sigma_\mathrm{s}}\right)_{n+1}-\left(\frac{h\gamma}{\sigma_\mathrm{s}}\right)_n,\quad(66)$$

$$\left(1-\frac{h\gamma}{\sigma_\mathrm{s}}\right)_\zeta=1-(1-\zeta)\left(\frac{h\gamma}{\sigma_\mathrm{s}}\right)_n-\zeta\left(\frac{h\gamma}{\sigma_\mathrm{s}}\right)_{n+1},$$

the incrementally advanced shear strain is obtained to be

$$\begin{aligned}
&\left(\frac{h\gamma}{\sigma_\mathrm{s}}\right)_{n+1}=\\
&=\frac{R_\Delta}{1+\zeta R_\Delta}+\left(1-\frac{R_\Delta}{1+\zeta R_\Delta}\right)\left(\frac{h\gamma}{\sigma_\mathrm{s}}\right)_n.
\end{aligned}\quad(67)$$

Results are shown in Fig. 13.

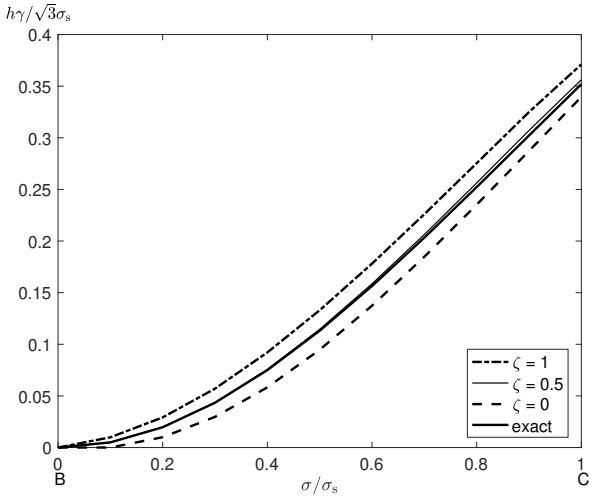

Figure 13: Incrementation of the shear strain in kinematic hardening along B–C. Source: created on behalf of the author.

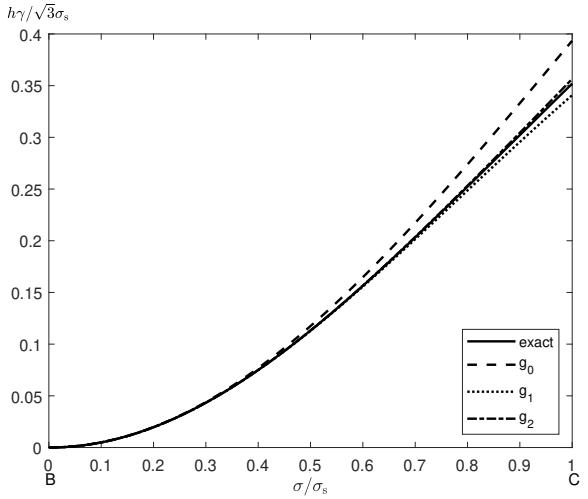

Figure 14: Successive analytical approximation of the shear strain in kinematic hardening along B–C. Source: created on behalf of the author.

5.2.2 Functional approach

The representation of the shear strain by an approximate function goes back to that of the axial strain. From eqn (63), adjusting the limits to the shear strain evolving from zero and carrying out the integration of the left-hand side,

$$\left(\frac{h\gamma}{\sigma_s}\right) = 1 - \exp(-R) = g\left(\frac{\sigma}{\sigma_s}\right). \tag{68}$$

The integral

$$\begin{aligned} R &= \int_0^{\frac{\sigma}{\sigma_s}} \left(\frac{\sigma}{\sigma_s} - \frac{h\eta}{\sigma_s}\right) \mathrm{d}\left(\frac{\sigma}{\sigma_s}\right) \\ &= \int_0^{\frac{\sigma}{\sigma_s}} \left[\frac{\sigma}{\sigma_s} - f\left(\frac{\sigma}{\sigma_s}\right)\right] \mathrm{d}\left(\frac{\sigma}{\sigma_s}\right) \end{aligned} \tag{69}$$

is evaluated for the function iterates f_i from eqn (62) that approximate the evolution of the axial strain. Thus eqn (68) gives for the shear strain the approximations

$$g_i\left(\frac{\sigma}{\sigma_s}\right) = 1 - \exp[-R(f_i)], \tag{70}$$

with the input

$$\begin{aligned} R_0 &= \frac{1}{2}\left(\frac{\sigma}{\sigma_s}\right)^2 \\ R_1 &= \frac{1}{2}\left(\frac{\sigma}{\sigma_s}\right)^2 - \frac{1}{12}\left(\frac{\sigma}{\sigma_s}\right)^4, \\ R_2 &= \frac{1}{2}\left(\frac{\sigma}{\sigma_s}\right)^2 - \frac{1}{12}\left(\frac{\sigma}{\sigma_s}\right)^4 \\ &+ \frac{2}{90}\left(\frac{\sigma}{\sigma_s}\right)^6 + \frac{1}{504}\left(\frac{\sigma}{\sigma_s}\right)^8, \\ R_3 &= \cdots. \end{aligned} \tag{71}$$

Fig. 14 demonstrates the successive approximation of the solution, eqn (35).

6 Conclusion

The plastic deformation of a thin-walled cylinder of circular cross-section has been considered for the isotropic- and the kinematic hardening hypothesis. In either case the analytical expressions are developed for the specific sequence of torsion and tension in question. The two hardening models are contrasted by the obtained solution. Assuming isotropic hardening tension does not affect previous twisting of the cylinder while kinematic hardening predicts the twist to diminish as observed in the laboratory.

Beyond the accomplishment of the analytical solution, the work extends to the exploration of approximate integration of the ordinary differential equation related to kinematic hardening in a certain branch of the loading program. Incremented numerical integration as well as analytical trials are seen to offer viable routes of successive approximation to the solution. Numerical limitations are found to conform with past experience.

The present study focuses on the development of solutions, closed-form and approximate, to this specific case with reference to a linearly hardening

material. Future work should explore the implications of nonlinear hardening.

Acknowledgement: Patrick Popa has produced the diagrams using Matlab.

References:

[1] M. Feigen, *Inelastic behavior under combined tension and torsion*, *Proc. 2nd USA Congr. of Appl. Mech.*, 1954, pp. 469–476.

[2] Iu.I. Kadashevich and V.V. Novozhilov, The theory of plasticity which takes into account residual microstresses (*PMM* Vol. 22, 1958, pp. 78–89) *TPMM*, Vol. 22, 1959, pp. 104–118.

[3] A.F. Kregers, Plastic strains under combined loading in tension and torsion, *Polymer Mechanics*, Vol. 2, 1966, pp. 12—16.

[4] A. Rusinko, Feigen's phenomenon in terms of the synthetic theory, *Int. Journal Engng. Research and Applications*, Vol. 4, No. 3, 2014, pp.172–180.

[5] A. Rusinko, and D. Fenyvesi, On the advantages of the theories of plasticity with singular loading surface, *Journal of Materials Science and Chemical Engineering*, Vol. 2, 2014, pp. 14–19.

[6] I. Doltsinis, *Elements of Plasticity*, 2nd Edition, WIT Press, Southampton 2010.

[7] D. W. A. Rees, Applications of classical plasticity theory to non-radial loading paths, *Proc. Royal Soc. London. A, Math. and Phys. Scs.* Vol. 410, No. 1839, 1987, pp. 443–475.

[8] R. Hill, *The Mathematical Theory of Plasticity*, Clarendon Press, Oxford 1950.

[9] W. Prager, A new method of analyzing stresses and strains in work-hardening plastic solids, *J. appl. Mech.* Vol.23, 1956, pp. 493-496.

[10] N.L. Doltsinis, Personal communication, ISST University of Muenster 2023.

[11] I. Doltsinis, *Large Deformation Processes of Solids*, WIT Press, Southampton 2012.

[12] *(text in German)* I.N. Bronstein and K.A. Semendjajew, *Taschenbuch der Mathematik*, 6. Auflage, Verlag Harri Deutsch, Zuerich und Frankfurt/M 1966.

Contribution of Individual Authors to the Creation of a Scientific Article (Ghostwriting Policy)

The author contributed in the present research, at all stages from the formulation of the problem to the final findings and solution.

Sources of Funding for Research Presented in a Scientific Article or Scientific Article Itself

No funding was received for conducting this study.

Conflict of Interest

The author has no conflict of interest to declare that is relevant to the content of this article.

Creative Commons Attribution License 4.0 (Attribution 4.0 International, CC BY 4.0)

This article is published under the terms of the Creative Commons Attribution License 4.0
https://creativecommons.org/licenses/by/4.0/deed.en_US